

IR Spectra and Properties of Solid Acetone, an Interstellar and Cometary Molecule

by

Reggie L. Hudson ^{a,*}, Perry A. Gerakines ^a, and Robert F. Ferrante ^b

^a Astrochemistry Laboratory, NASA Goddard Space Flight Center, Greenbelt, MD, 20771 USA

^b Chemistry Department, U.S. Naval Academy, Annapolis, MD 21402 USA

ABSTRACT

Mid-infrared spectra of amorphous and crystalline acetone are presented along with measurements of the refractive index and density for both forms of the compound. Infrared band strengths are reported for the first time for amorphous and crystalline acetone, along with IR optical constants. Vapor pressures and a sublimation enthalpy for crystalline acetone also are reported. Positions of ¹³C-labeled acetone are measured. Band strengths are compared to gas-phase values and to the results of a density-functional calculation. A 73% error in previous work is identified and corrected.

Keywords: IR spectroscopy, band strengths, astrochemistry, amorphous solids, ices

* Corresponding author.

E-mail address: reggie.hudson@nasa.gov (R. L. Hudson).

1. Introduction

Among the roughly 200 extraterrestrial molecules identified, there are at least two members of nearly every type of common organic compound, such as alkanes, alkenes, alkynes, aromatics, alcohols, amines, nitriles, ethers, epoxides, and mercaptans (thiols). From the carbonyl-containing classes, there are at least two interstellar identifications each of common aldehydes, esters, acids, and amides. The lone exception is the ketones, for which only acetone, the prototypical ketone, has been identified.

Our interest in solid acetone arises from its possible role as a degradation product of propylene oxide, a recently discovered interstellar molecule.¹ However, solid acetone is of interest in itself as it has been detected both in the interstellar medium and on the surface of a comet.^{2,3} The reactions for the formation and destruction of acetone are unclear, but although they almost certainly involve solid-phase chemistry the lack of quantitative data on solid acetone hinders studies of this molecule.

An example of the problems to which a lack of acetone data can lead is found in a recent paper on the irradiation of acetone ices at 16 K.⁴ Lacking solid-phase IR band strengths, the authors used the results of a density-functional theory (DFT-B3LYP) calculation by others⁵ to estimate the thickness of their acetone samples. Here we show that that approach led to a 73% error in acetone abundance, which propagated through the authors' subsequent work on product abundances, reaction cross sections, and an attempt at a mass-balance calculation. Moreover, the phase or state of the authors' acetone ices was not given and there is little in the literature with which to compare.

In the present paper we present new mid-infrared spectra of amorphous and crystalline acetone along with band strengths and optical constants. We also report measurements of a refractive index and density for both forms of the compound. As an example of one use of this new information, we have measured vapor pressures and a sublimation enthalpy for crystalline acetone. IR positions of ¹³C-labeled acetone also have been measured, apparently for the first time. Band strength results are compared to gas-phase values and a density-functional calculation. These new results will be useful to laboratory astrochemists and others studying the formation and reactions of acetone in a variety of extraterrestrial environments.

2. Experimental

Most of our procedures and equipment can be found in our recent papers, and so only a summary is given here.⁶

All samples were prepared by vapor-phase condensation onto a KBr substrate (area $\approx 5 \text{ cm}^2$) precooled within a vacuum system ($\sim 10^{-8}$ - 10^{-10} torr). Depositions were at ~ 10 K to make amorphous samples and at ~ 125 K to make crystalline ones, usually at a

rate that gave a growth in ice thickness of about $1 \mu\text{m hr}^{-1}$ as measured with interference fringes. Transmission IR spectra were recorded with a Thermo iS50 spectrometer using an unpolarized IR beam aligned perpendicular to the ice's surface. Spectra typically were recorded from 4000 to 400 cm^{-1} using 200 scans at 1-cm^{-1} resolution.

Solid acetone's density (ρ) and refractive index (n) were measured inside a stainless-steel ultra-high vacuum (UHV) chamber ($\sim 10^{-10}$ torr). Ices were grown on the gold-coated surface of an INFICON quartz-crystal microbalance (QCM) for density measurements.⁶ During the growth of each ice, two 670-nm lasers generated interference fringes from the surface of the substrate. Measuring the period of each laser's fringes allowed the calculation of n in the usual way. Again, see our earlier papers or, from another laboratory, the work of Satorre et al.⁷ As a check on our work, we also measured n_{670} with the two-laser interferometer we have used in the past.⁸ Results from the two systems agreed within experimental error. Both systems also were interfaced to IR spectrometers so that the phase and quality of each ice sample could be checked.

Acetone and acetone-2-¹³C (carbonyl position labeled) were purchased from Sigma Aldrich and degassed with liquid nitrogen and freeze-pump-thaw cycles before use.

3. Results

3.1. Refractive Indices and Densities

Refractive indices at 670 nm (n_{670}) were measured in triplicate and gave $n_{670} = 1.335$ for amorphous acetone at 20 K and $n_{670} = 1.453$ for crystalline acetone at 125 K, with a standard error of about ± 0.002 in each case. Measurements of density (ρ) resulted in values of 0.783 and 0.999 g cm^{-3} for amorphous and crystalline acetone, respectively, with a standard error of about $\pm 0.002 \text{ g cm}^{-3}$ for each value. For comparison to amorphous acetone, the liquid state has $n_D = 1.356$ and $\rho = 0.784 \text{ g cm}^{-3}$ at $25 \text{ }^\circ\text{C}$.⁹ Diffraction studies give the density of crystalline acetone as 0.987 g cm^{-3} .¹⁰

3.2. Infrared Spectra and Band Strengths

To check that our spectra were neither saturated nor resolution limited, IR spectra were first recorded for ice thicknesses up to $4 \mu\text{m}$ and resolutions up to 0.5 cm^{-1} . Since little change was found beyond 1 cm^{-1} , that resolution was used in most of our work.

Figure 1 shows survey spectra of acetone deposited at 10 K to make an amorphous solid and at 125 K to make a crystalline one, the latter as indicated by the increase in splitting of peaks on going from (a) to (b) and the decrease in widths of several bands. Peak positions for the two traces are similar, but there are differences in relative intensities. Table 1 lists positions of selected IR peaks in our spectra of amorphous and

crystalline acetone in Figure 1, along with some literature results for comparison. Assignments to specific modes are taken from gas-phase studies¹¹ and are, of course, approximations for these solids. Mixing is expected as are factor-group splittings. Although crystalline acetone has little direct relevance to the study of extraterrestrial ices, recent work by our group has uncovered confusion in the literature involving IR spectra of solid N₂O, C₂H₂, C₂H₄, CH₄, CO₂, CH₃SH, and C₂H₅OH, all molecules of astrochemical interest, emphasizing the importance of having reference spectra for both non-crystalline and crystalline solids.^{6,8,12,13,14,15,16}

Figures 2 and 3 have spectra for the same two ices as in Figure 1, but traces (b) and (c) show the effect of warming the amorphous sample that was initially at 10 K. Trace (b) in each figure shows that little change was seen on warming from 10 to 80 K. Continued warming to 97 K and holding there for about 30 seconds resulted in irreversible sharpening, splitting, and shifts in many IR bands, indicative of the amorphous sample's crystallization, as seen in trace (c) in both figures. – Infrared spectra have been used to record such phase changes with temperature since at least the 1950s.^{17,18} – The bands at 1400 -1100 cm⁻¹ undergo particularly pronounced changes on warming the ice from 10 K, being much stronger in the sample warmed to 97 K, trace (c), than in the ice made at 125 K, trace (d). Similarities in peak positions, but differences in intensities, suggest that the ice made by warming from 10 K resembled, but was not identical to, the one made at 125 K. Warming the initially amorphous ice beyond the 97 K of Figures 1 and 2 gave slight, if any, additional changes in relative intensities. We note that the crystallization observed on going from 80 to 97 K was kinetically driven and could also be brought about by holding an amorphous sample overnight at 90 K. All of our samples underwent rapid sublimation at 150 K, to the extent that results at and above that temperature were unreliable.

Depositions to give ices of different thicknesses, and measurements of the corresponding IR band areas, allowed Beer's law plots to be prepared in the usual way.¹⁹ Figure 4 shows three examples. All such graphs had correlation coefficients greater than or equal to 0.99. After converting from absorbance to optical depth (= 2.303 × absorbance), the apparent band strengths (*A'*) of Table 2 were obtained for selected regions of the IR spectra of amorphous and crystalline acetone. The only *A'* values we have found in the literature also are included in Table 2, with the spectral regions chosen to match those in one of the earlier papers.²⁰ As in our work on hydrocarbons, we estimate that uncertainties in *A'* are no greater than about 5%, and probably much lower given the small uncertainties in ρ and n_{670} .¹²

An unexpected observation in our work involved the shape of crystalline acetone's carbonyl stretching band near 1700 cm⁻¹. The upper panel of Figure 5 shows that on going from (a) to (b) to (c), with ice thickness rising from about 0.46 to 0.63 to 0.92 μm, the height of the 1715-cm⁻¹ peak increased relative to the 1708-cm⁻¹ peak. Conversely, as we warmed our thickest sample to where it began to sublime and become thinner, the shape of the carbonyl band for the 0.92-μm ice (c) also changed. This is shown in Figure 5's spectrum (d), which was from the same sample as in (c), but after sitting at 125 K for about 20 hours. As the ice became thinner, the 1715-cm⁻¹ peak became

smaller relative to the 1708-cm^{-1} peak, the reverse of the (a)-to-(c) sequence. No other IR feature of crystalline acetone displayed comparable behavior.

Infrared positions for acetone- d_6 have been published²¹ but we are unaware of data for ^{13}C -labeled acetone. Therefore, in Table 3 we list some of the peaks observed for amorphous and crystalline acetone- $2\text{-}^{13}\text{C}$ at 10 K. In general, the ^{13}C isotopic shifts were about as expected, such as a shift of $\sim 40\text{ cm}^{-1}$ for the carbonyl stretch (ν_3).²² The peaks listed in Table 3 were helpful in identifying several small ^{13}C features in the spectrum of unlabeled acetone, such as the one near 1668 cm^{-1} in Figure 5.

Most of our depositions were at 10 - 20 K to make amorphous ices or 125 K to make crystalline ones. However, a few depositions were made at 77 K, and the resulting spectra appeared to have both amorphous and crystalline components. Subsequent warming always gave the same spectrum as produced by a 125-K deposition, the upper trace in Figure 1.

A few spectra were recorded with the acetone sample and substrate rotated 10 - 20° about an axis perpendicular to the IR beam, so as to check for possible longitudinal optical (LO) bands. None were found.

3.3. Optical Constants

To test our results and better quantify them, we also calculated mid-IR optical constants, n and k , for amorphous and crystalline acetone using an iterative Kramers-Kronig method.²³ Figures 6 and 7 show the results. The optical constants for crystalline acetone then were used to calculate the spectrum of crystalline acetone for three different ice thicknesses. The results for the carbonyl region are shown in Figure 5's lower panel.

3.4. Vapor Pressures

Warming solid acetone to 125 K and above resulted in its sublimation. Infrared spectra recorded over time at 125 to 140 K gave vapor pressures for crystalline acetone by the method of Khanna et al.²⁴ From vapor pressures, in mPa, of 9.41 (125 K), 59.0 (130 K), 288 (135 K), and 1190 (140 K), a Clapeyron plot was constructed (correlation coefficient = 0.999), and from its slope a sublimation enthalpy of 47 kJ mol^{-1} was found, close to an earlier result for a similar, but not identical, measurement.²⁵ Note that our vapor pressures could only be calculated after the band strengths (A' values) of Table 2 were known, which in turn required measurements of both n_{670} and ρ (Section 3.1).

4. Discussion

Amorphous organic solids can be considered as having similarities in structure to the corresponding liquids. Therefore, it is not surprising that the IR spectrum of amorphous acetone at 10 K in Figures 1 - 3 resembles that of liquid acetone in standard spectral compilations such as the Aldrich atlas.²⁶ The strongest features in both cases are the carbonyl band ($\sim 1711\text{ cm}^{-1}$) followed by a CH_3 symmetric deformation (1364 cm^{-1}) and the CCC asymmetric stretch (1229 cm^{-1}). Rounded band shapes are found in both the liquid and amorphous acetone spectra, with little or none of the sharp splitting common with crystalline solids.

Turning to crystalline acetone, the work closest to ours in the procedures used is that of Ioppolo et al.²⁷ Their sample was prepared, and presumably its spectrum was recorded, at 150 K, a temperature difficult for us to reach due to the sublimation already mentioned. The bottom trace of their Figure 3 is for crystalline acetone and, like our work, shows that the carbonyl feature strongly dominates the spectrum, with about four regions of less intense, but sharp, features at $1500 - 1000\text{ cm}^{-1}$. More-detailed comparisons are difficult as no deposition rate, spectral resolution, or ice thickness was provided, the sample was tilted at an angle of 45° to the incident IR beam, and no enlargements of individual features were shown. Nevertheless, our agreement with this earlier study appears to be satisfactory.

Comparisons of our acetone spectra to other previous work are more difficult as no unequivocal comparison spectra were found in the literature. The spectrum of Andrade et al.⁴ was not explicitly stated to be for an amorphous ice, and the comparison those authors used was to ices described as polycrystalline. The latter spectra, in turn, were for samples of Harris and Levin²⁸ made at 77 K, which our measurements showed could contain both amorphous and crystalline components. However, since our Table 1 shows good agreement between our data and that in the two earlier papers, we interpret the results of Andrade et al. as referring to an amorphous ice, while those of Harris and Levin are for an acetone sample that was highly crystalline. One exception to our agreement with previous work is the IR peak seen near 1035 cm^{-1} by Andrade et al. for amorphous acetone. We did not find this feature either in any of our spectra or in those of earlier publications. It is not known if it was from an instrumental artifact, contamination, or something else.

Still other spectra of solid acetone have been published, but all were recorded under conditions different from ours. Krause et al.²⁹ published extensive data on acetone crystals grown between salt plates and showing orientation effects. Our results for crystalline acetone appear to agree, to the extent comparisons are valid, with theirs. Shin et al.³⁰ reported spectra of the carbonyl region of solid acetone sandwiched between layers of H_2O -ice at 120 K. Their spectra for that one band resemble ours for crystalline acetone, at least qualitatively, and appear to show a thickness dependence resembling that in our Figure 5. Richardson³¹ studied acetone adsorbed on NaCl that had itself been sublimed onto a substrate, but his samples were not identified as either amorphous or crystalline. Assuming that they were amorphous then his results appear

to agree with ours. Finally, Schaff and Roberts³² reported that acetone adsorbed onto amorphous H₂O-ice showed a thickness dependence for its carbonyl feature's position, which seems to resemble the trend in our Figure 5, but full spectra were not shown and the ice thicknesses used were much smaller than ours.

None of the earlier papers on solid acetone contained measurements of band strengths, and so direct comparisons to our A' values are impossible. As an alternative, Figure 8 compares our amorphous-acetone band strengths to values measured for crystalline acetone, values measured for gas-phase acetone, and a set of calculated values for gas-phase acetone, all taken from Table 2. No single correlation appears to be better than the other two, and so none can be recommended as an alternative to direct measurements on the amorphous solid. The crystalline-phase band strengths vary from the amorphous-acetone values by 0 to 54%, the variations of the gas-phase values from ours on amorphous acetone range from 10 to 99%, and the differences in the calculated (DFT method) results and our work are 0 to 143%.⁵ The red diamond in Figure 8 is for the IR feature used by Andrade et al.⁴ as a reference, acetone's CCC asymmetric stretch at 1229 cm⁻¹. Its calculated A' value differs by 73% from our measurements, introducing an error of 73% in the initial abundance of amorphous acetone calculated by Andrade et al., which carried through those authors' subsequent determinations of product abundances, kinetics results, and mass balance calculation. We should point out Katsyuba et al. have shown that DFT calculations of IR intensities are much more accurate for isolated molecules than for those in condensed phases.³³ Our acetone work agrees with that conclusion.

Returning to our Figure 5 for crystalline acetone, we first suspected that the thickness trend shown was due to variations in the temperature or rate at which ices were grown. However, depositions at multiple temperatures and rates failed to give the changes in band shapes seen in Figure 5. Acetone has a crystalline-crystalline phase change around 127 K³⁴, but that too seemed not to be a factor as only one crystalline phase appeared to be present in our samples. For now we favor an explanation based on crystalline acetone's IR optical constants, n and k since spectra calculated (bottom of Figure 5) agreed well with the observed spectra (top of Figure 5). This interpretation also agrees with our previous work⁸ with crystalline acetylene (C₂H₂), which showed that the two peaks of that solid's IR spectrum near 770 and 761 cm⁻¹ displayed a behavior resembling that of crystalline acetone in Figure 5. Even earlier, Khanna and co-workers found a similar behavior for crystalline SO₂'s IR features at 1323 and 1310 cm⁻¹.³⁵ For both C₂H₂ and SO₂, spectra calculated from the compound's optical constants matched the observations. Again, our Figure 5 shows close agreement between calculated and observed shapes for crystalline acetone's carbonyl feature using only one set of optical constants.

We end this section by returning to Figure 3. Traces (c) and (d) show that there are differences, particularly in relative band intensities, between the spectra of crystalline acetone made by warming from 10 K and by depositing at 125 K. Similar differences have been reported for other icy solids, such as H₂O, but otherwise have received little attention.³⁶ It is tempting to postulate factors such as rotational conformations, the rate

of crystal growth, or unidentified solid phases as contributing to these spectral differences, but instead we leave them for future investigations. There may well be metastable or intermediate phases of solid acetone awaiting discovery.

5. Summary and Conclusions

In this paper we have reported measurements of several physical properties that will be useful in work on solid acetone by laboratory astrochemists and others. This new information includes a refractive index for use in measuring ice thicknesses, vapor pressures, and an energy of sublimation. The band strengths in our Table 2 can help in determining the column density of acetone samples, facilitating lab-to-lab comparisons. The mass densities we report are useful in the calculations of the stopping power of various types of ionizing radiation. Our IR spectra and isotopic shifts can aid in the analyses of acetone-containing ices in a variety of photo- and radiation chemistry experiments on astrochemical ice analogs. Just as important, to our knowledge Figures 1 through 3 are the first presentations of the mid-IR spectra of amorphous and crystalline acetone, prepared in a single laboratory with the same equipment and accompanied by the sample's thickness (IR pathlength). The optical constants we have measured can be used to simulate the IR spectra of acetone under a variety of conditions, such as transmission and reflection. Finally, our results also could be used to estimate the level of acetone contamination in icy solids.

Acknowledgements

This work was supported by the NASA Astrobiology Institute through funding awarded to the Goddard Center for Astrobiology under proposal 13-13NAI7-0032. Marla Moore and Sarah Frail assisted with some of the measurements. Mark Loeffler is acknowledged for construction and testing of the UHV chamber. An anonymous reviewer is thanked for bringing the crystalline acetone spectrum of Ioppolo et al.²⁷ to our attention.

References

- ¹ B. A. McGuire, P. B. Carroll, R. A. Loomis, I. A. Finneran, P. R. Jewell, A. J. Remijan, G. A. Blake, Discovery of the interstellar chiral molecule propylene oxide (CH₃CHCH₂O), *Science* 352 (2016) 1449.
- ² L. E. Snyder, F. J. Lovas, D. M. Mehringer, N. Y. Miao, Y.-J. Kuan, J. M. Hollis, P. R. Jewell, Confirmation of interstellar acetone, *Astrophys. J.* 578 (2002) 245.

- ³ K. Altwegg, H. Balsiger, J. J. Berthelier, A. Bieler, et al., Organics in comet 67P – A first comparative analysis of mass spectra from ROSINA–DFMS, COSAC and Ptolemy, *Mon. Not. R. Astron. Soc.* 469 (2017) S130.
- ⁴ D. P. P. Andrade, A. L. F. de Barross, J. Ding, H. Rothard, P. Boduch, E. F. da Silveira, Acetone degradation by cosmic rays in the solar neighbourhood and in the Galactic Centre, *Mon. Not. R. Astron. Soc.* 444 (2014) 3792.
- ⁵ C. J. Bennett, S. Chen, B. Sun, A. H. H. Chang, R. I. Kaiser, Mechanical studies on the irradiation of methanol in extraterrestrial ices, *Astrophys. J.* 660 (2007) 1588.
- ⁶ R. L. Hudson, M. J. Loeffler, P. A. Gerakines, Infrared spectra and band strengths of amorphous and crystalline N₂O, *J. Chem. Phys.* 146 (2017) 0243304.
- ⁷ M. A. Satorre, M. Domingo, C. Millán, R. Luna, R. Vilaplana, C. Santonja, Density of CH₄, N₂ and CO₂ ices at different temperatures of deposition, *Planet. Space Sci.* 56 (2008) 1748.
- ⁸ R. L. Hudson, R. F. Ferrante, M. H. Moore, Infrared spectra and optical constants of astronomical ices: I. Amorphous and crystalline acetylene, *Icarus* 228 (2014) 276.
- ⁹ B. Orge, M. Iglesias, J. Tojo, J. L. Legidot, Densities and refractive indices of acetone + methanol + 2-methyl-2-butanol at 298.15 K, *J. Chem. Eng. Ref. Data* 40 (1995) 1199.
- ¹⁰ D. R. Allan, S. J. Clark, R. M. Ibberson, S. Parson, C. R. Pulham, L. Sawyer, The influence of pressure and temperature on the crystal structure of acetone, *Chem. Comm.* (1999) 751.
- ¹¹ G. Dellepiane, J. Overend, Vibrational spectra and assignment of acetone, $\alpha\alpha\alpha$ acetone-d₃ and acetone d₆, *Spectrochim. Acta* 22 (1966) 593.
- ¹² R. L. Hudson, P. A. Gerakines, M. H. Moore, Infrared spectra and optical constants of astronomical ices: II. Ethane and ethylene, *Icarus* 243 (2014) 148.
- ¹³ P. A. Gerakines, R. L. Hudson, The infrared spectra and optical constants of elusive amorphous methane, *Astrophys. J.* 805 (2015) L20.
- ¹⁴ P. A. Gerakines, R. L. Hudson, First infrared band strengths for amorphous CO₂, an overlooked component of interstellar ices, *Astrophys. J.* 808 (2015) L40.
- ¹⁵ R. L. Hudson, Infrared spectra and band strengths of CH₃SH, an interstellar molecule, *Phys. Chem. Chem. Phys.* 18 (2016), 25756.

- ¹⁶ R. L. Hudson, An IR investigation of solid amorphous ethanol - Spectra, properties, and phase changes, *Spectrochim. Acta* 187 (2017) 82.
- ¹⁷ F. E. Mahlerbe, H. J. Bernstein, Infrared spectra of rapidly solidified vapors, *J. Chem. Phys.* 19 (1951) 1607.
- ¹⁸ R. E. Nightingale, E. L. Wagner, The vibrational spectra and structure of solid hydroxylamine and deuterio-hydroxylamine, *J. Chem. Phys.* 22 (1954) 203.
- ¹⁹ J. Hollenberg, D. A. Dows, Measurement of absolute infrared absorption intensities in crystals, *J. Chem. Phys.* 34 (1961) 1061.
- ²⁰ J. D. Rogers, B. Rub, S. Goldman, W. B. Person, Measurement of infrared intensities for fundamental vibrations of gaseous acetone, *J. Phys. Chem.* 85 (1981) 3727.
- ²¹ R. H. Mann, W. B. Dixon, Comprehensive Urey-Bradley Force Field for Molecules with Geminal Methyl Groups. I. Acetone, *J. Chem. Phys.* 57 (1972) 792.
- ²² M. Hawkins, L. Andrews, Reactions of atomic oxygen with ethene in solid argon. The infrared spectrum of vinyl alcohol, *J. Amer. Chem. Soc.* 105 (1983) 2523.
- ²³ M. H. Moore, R. F. Ferrante, W. J. Moore, R. L. Hudson, Infrared spectra and optical constants of nitrile ices relevant to Titan's atmosphere, *Astrophys. J. Suppl. Ser.* 191 (2010) 96.
- ²⁴ R. K. Khanna, J. E. Allen Jr, C. M. Masterson, G. Zhao, Thin-film infrared spectroscopic method for low-temperature vapor pressure measurements, *J. Phys. Chem.* 94 (1990) 440.
- ²⁵ F. Dominé, L. Rey-Hanot, Adsorption isotherms of acetone on ice between 193 and 213 K, *Geophys. Res. Lett.* 29 (2002) 20-1.
- ²⁶ C. J. Pouchert, *The Aldrich Library of FT-IR Spectra*, 2nd edition (Milwaukee: Aldrich), 1985, 405.
- ²⁷ S. Ioppolo, B. A. McGuire, M. A. Allodi, G. A. Blake, THz and mid-IR spectroscopy of interstellar ice analogs: Methyl and carboxylic acid groups, *Trans. Farad. Soc.*, 168, 2014, 461.
- ²⁸ W. C. Harris, I. W. Levin, Raman spectrum of polycrystalline acetone and acetone-d₆, Harris and Levin's Raman paper, *J. Molec. Spec.* 43 (1972) 117.
- ²⁹ P. F. Krause, B. G. Glagola, J. E. Katon, Polarized infrared spectrum of crystalline acetone, *J. Chem. Phys.* 61 (1974) 5331.

- ³⁰ S. Shin, H. Kang, J. S. Kim, H. Kang, Phase transitions of amorphous solid acetone in confined geometry investigated by reflection absorption infrared spectroscopy, *J. Phys. Chem. B* 118 (2014) 13349.
- ³¹ H. H. Richardson, Infrared spectroscopy and photochemistry of acetone adsorbed on sodium chloride films, *J. Phys. Chem.* 96 (1992) 5898.
- ³² J. E. Schaff, J. T. Roberts, Toward an understanding of the surface chemical properties of ice: Differences between the amorphous and crystalline surfaces, *J. Phys. Chem.* 100 (1996) 14151.
- ³³ S. A. Katsyuba, E. E. Zvereva, T. I. Burganov, Is there a simple way to reliable simulations of infrared spectra of organic compounds?, *J. Phys. Chem. A*, 117 (2013) 6664.
- ³⁴ R. M. Ibberson, W. I. F. David, O. Yamamuro, Y. Miyoshi, T. Matsuo, H. Suga, Calorimetric, dielectric, and neutron diffraction studies on phase transitions in ordinary and deuterated acetone crystals, *J. Phys. Chem.* 99 (1995) 14167.
- ³⁵ R. K. Khanna, G. Zhao, M. J. Ospina, J. C. Pearl, Crystalline sulfur dioxide: crystal field splittings, absolute band intensities, and complex refractive indices derived from infra-red spectra, *Spectrochim. Acta* 44A (1988) 581.
- ³⁶ M. H., Moore, R. L. Hudson, P. A. Gerakines, P. A. (2001). Mid- and far-infrared spectroscopic studies of the influence of temperature, uv photolysis and ion bombardment on cosmic-type ices, *Spectrochim. Acta* 57A (2001) 843.

Table 1

Positions of Some Acetone Vibrations

Mode ν	Approximate motion	Amorphous, 10 K IR ^a	Crystalline 125 K IR ^a	Solid 13 K IR ^b	Solid 77 K Raman ^c
ν_{13}	CH ₃ asymm stretch	3002.0	3002.9	3001.8	3004.0
ν_1	CH ₃ asymm stretch	3002.0	2999.0	3001.8	3004.0
ν_9	CH ₃ asymm stretch	2967.4	2969.3	2967.0	2972.0
ν_{20}	CH ₃ asymm stretch	2967.4	2969.3	2967.9	2972.0
ν_2	CH ₃ symm stretch	2920.5	2921.5	2919.7	2920.0
ν_{14}	CH ₃ symm stretch	2920.5	2918.4	2919.7	2920.0
ν_3	C=O stretch	1711.4	1715.2, 1708.1, 1704.8, 1698.8	1711.0	1697.0
ν_{21}	CH ₃ asymm def	1441.6	1442.8, 1439.8	1441.9	1444.0
ν_{10}	CH ₃ asymm def	----	1433.8	----	1431.0
ν_4	CH ₃ asymm def	1418.9	1418.7	1419.1	1426.0
ν_{15}	CH ₃ asymm def	----	1403.2	----	1408.0
ν_{16}	CH ₃ symm def	1364.4	1360.9	1364.0	1366.0
ν_5	CH ₃ symm def	1350.8	1350.3, 1346.8	1351.8	1351.0
ν_{17}	CCC asymm stretch	1228.9	1234.0	1229.5	1229.0
ν_{22}	CH ₃ rock	1095.6	1098.5	1096.0	1098.0
ν_6	CH ₃ rock	1071.4	1072.0 ^d	1070.0	1072.0
ν_{18}	CH ₃ rock	897.3	907.2	897.9	905.0
ν_{11}	CH ₃ rock	871.0	873.4	872.3	872.0
ν_7	CCC symm stretch	791.2	793.9	791.1	796.0
ν_{19}	CO in-plane def	533.6	533.7	----	533.0
ν_8	CCC scissoring	----	----	----	497.0
ν_{23}	CO out-of-plane def	----	----	----	402.0
ν_{24}	torsional	----	----	----	130.0
ν_{12}	torsional	----	----	----	112.0

^a This work; assignments at 1500 - 1400 cm⁻¹ are somewhat uncertain ^b From Andrade et al.⁴ arranged to correspond to modes (ν) in the first column, but with the authors' peak near 1035 cm⁻¹ omitted ^c From Harris and Levin²⁸ ^d Broad feature.

Table 2
IR Band Strengths (A') of Acetone ^a

Region (cm^{-1})	Approximate Motion	Amorphous 10 K ^b	Crystalline 125 K ^b	Gas Phase ^c	DFT Calculation ^d
3100 - 2800	-CH ₃ stretches	3.90	1.78	7.31	9.46
1740 - 1680	C=O stretch	26.7	28.6	24.1	29.00
1500 - 1380	-CH ₃ deformation	9.19	9.23	5.81	8.59
1380 - 1335	-CH ₃ deformation	13.9	9.32	11.5	13.90
1250 - 1210	CCC asymmetric stretch	7.35	4.38	11.0	12.70
1100 - 1080	-CH ₃ rocking	1.57	2.17	0.747	0.52
940 - 840	-CH ₃ rocking	0.832	0.721	1.26	1.58
820 - 760	CCC symmetric stretch	0.159	0.213	0.316	0.25
545 - 524	CO in-plane deformation	2.13	1.70	2.82	2.54

^a Units are 10^{-18} cm molecule⁻¹ ^b This work, with uncertainties of ~5% ^c From Rogers et al.²⁰ ^d From Bennett et al.⁵

Table 3

IR Positions of Amorphous and
Crystalline Acetone-2-¹³C

Mode ν	Amorphous 10 K ^a	Crystalline 125 K ^a
v13	3001.8	3002.4
v1	3001.8	2998.9
v9	2967.4	2969.3
v20	2967.4	2969.3
v2	2920.0	2920.8
v14	2920.0	2920.8
v3	1672.5	1676.4, 1669.0, 1666.1, 1660.3
v21	1438.9	1440.0
v10	----	----
v4	1417.0	1418.3
v15	----	----
v16	1358.8	1350.8
v5	1349.7 ^b	1347.3
v17	1203.0	1207.9
v22	1082.4	1085.3
v6	----	----
v18	894.4	904.2
v11	871.0	873.4
v7	790.1	792.0
v19	532.2	532.0

^a Assignments at 1500 - 1400 cm⁻¹ are somewhat uncertain ^b Poorly resolved.

Figures

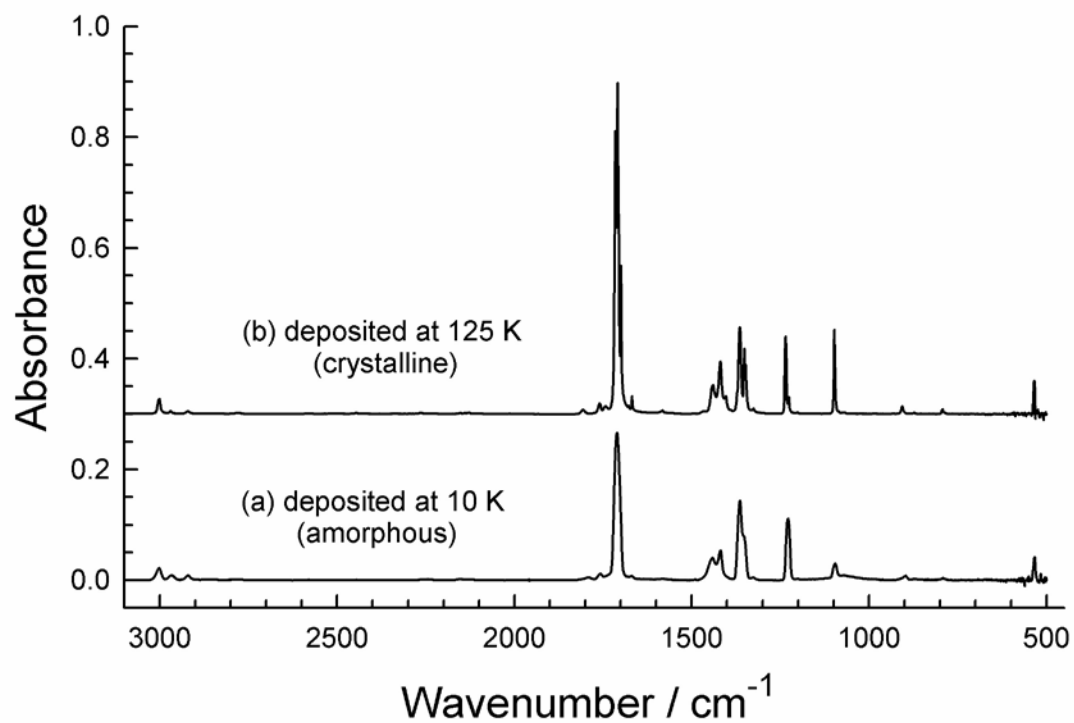


Figure 1. Survey infrared spectra of acetone deposited at (a) 10 and (b) 125 K. Spectra were recorded at the temperature of deposition and have been offset for clarity. Initial thicknesses were about 0.5 and 0.6 μm for the 10 and 125 K ices, respectively.

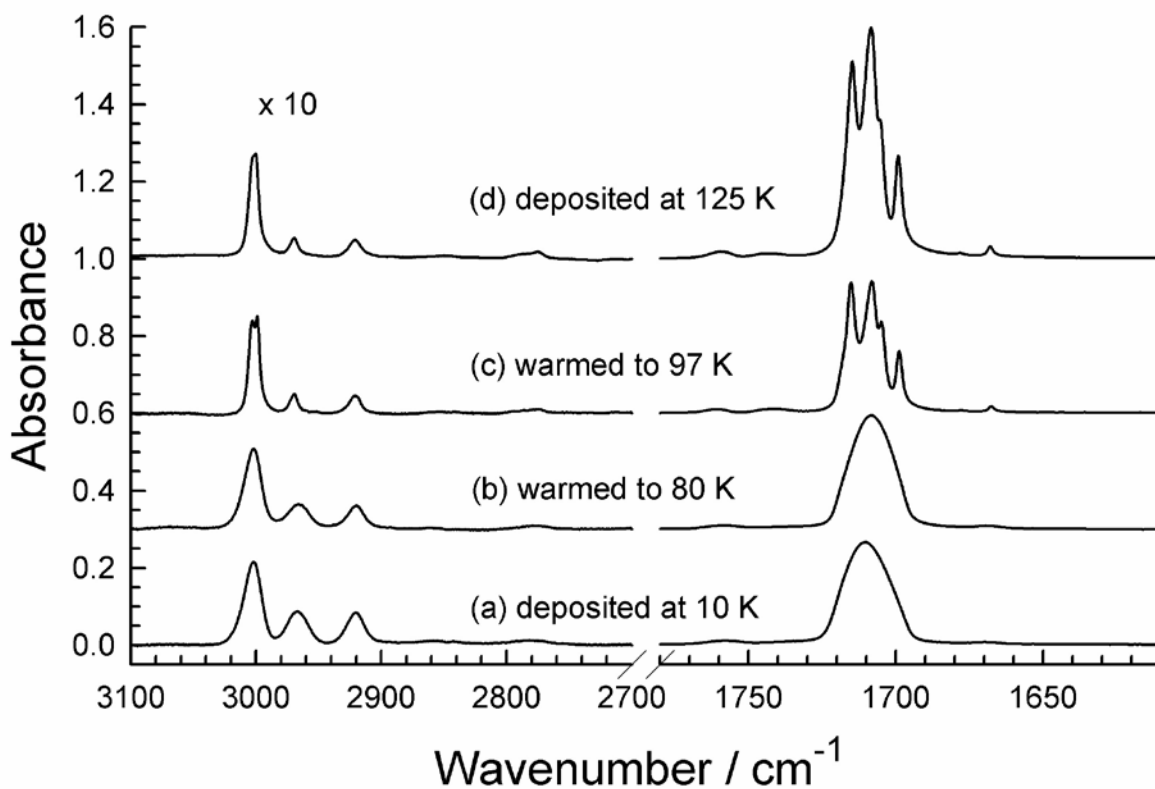


Figure 2. Infrared spectra of acetone deposited at 10 K and warmed to 80 and 97 K compared to a spectrum of acetone deposited at 125 K. Note the vertical expansion factor of 10 on the left. Spectra have been offset for clarity. Initial thicknesses were about 0.5 and 0.6 μm for the 10 and 125 K ices, respectively.

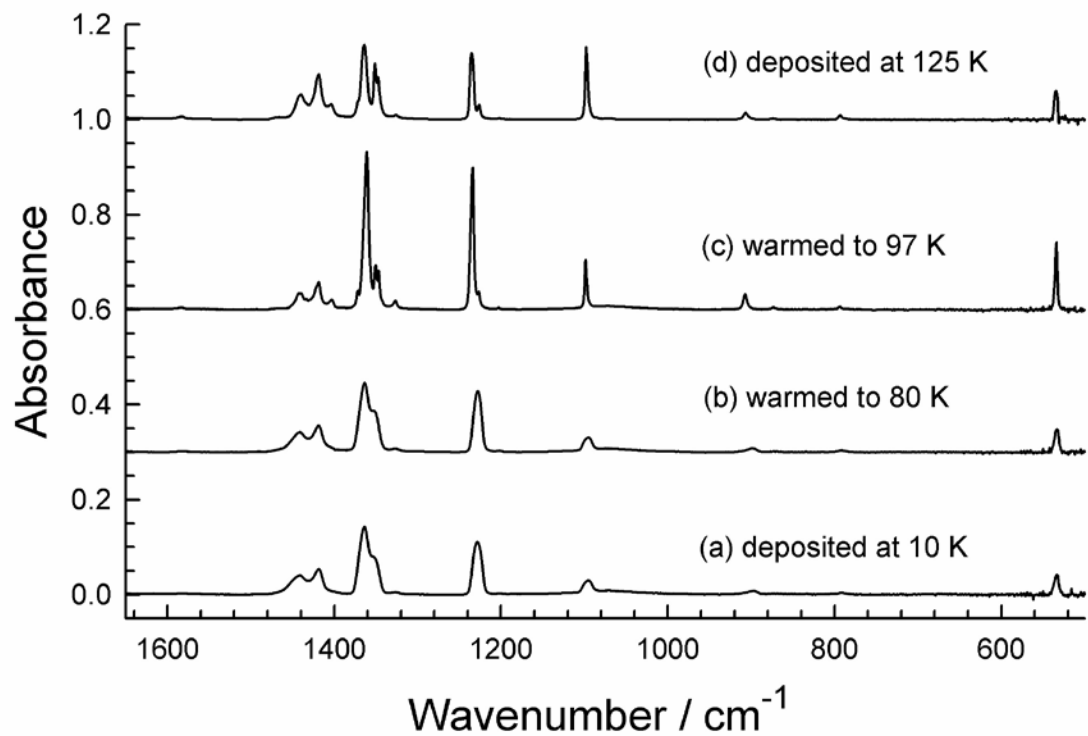


Figure 3. Continuation of Figure 2 showing the 1600 - 500 cm^{-1} region. Spectra have been offset for clarity. Initial thicknesses were about 0.5 and 0.6 μm for the 10 and 125 K ices, respectively.

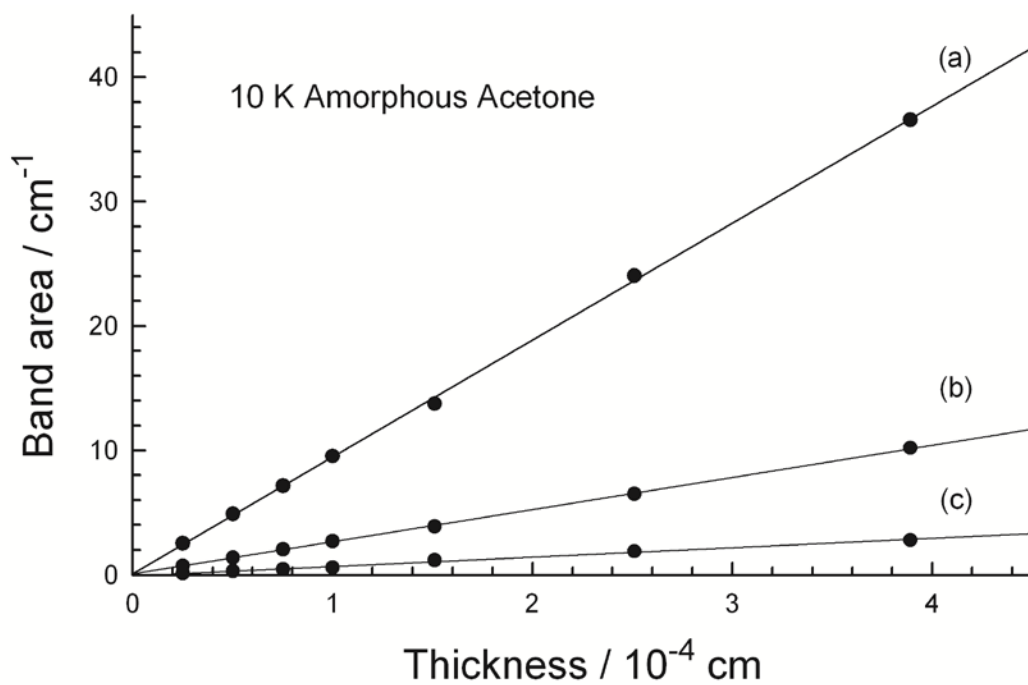


Figure 4. Beer's law plots for 10 K amorphous acetone. Integrations were for the IR features (a) ν_3 at 1740 - 1680 cm^{-1} , (b) ν_{17} at 1215 - 1210 cm^{-1} , and (c) ν_{19} at 545 - 524 cm^{-1} .

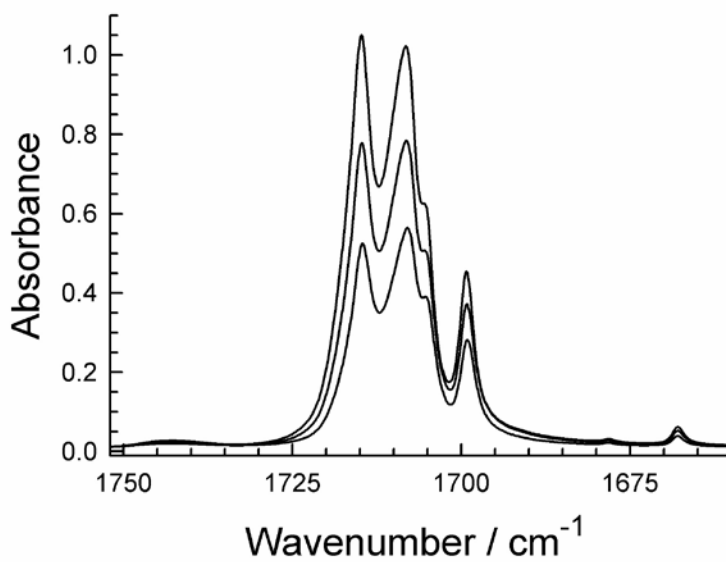
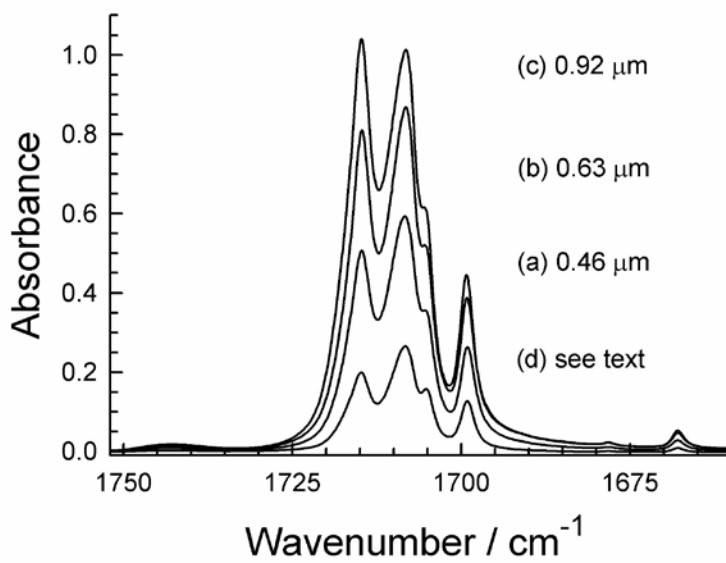


Figure 5. Upper: Carbonyl region of the IR spectra of 125-K crystalline acetone ices with initial thicknesses of approximately (a) 0.46, (b) 0.63, and (c) 0.92 μm . Spectrum (d) was recorded after the ice of (c) had sat about 20 hours at 125 K. Lower: Spectra calculated for thicknesses of (a) 0.46, (b) 0.63, and (c) 0.92 μm using the optical constants of crystalline acetone.

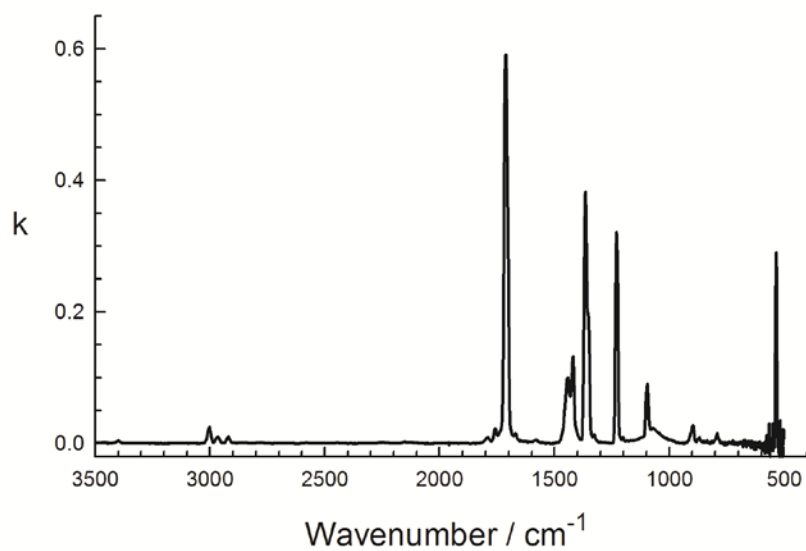
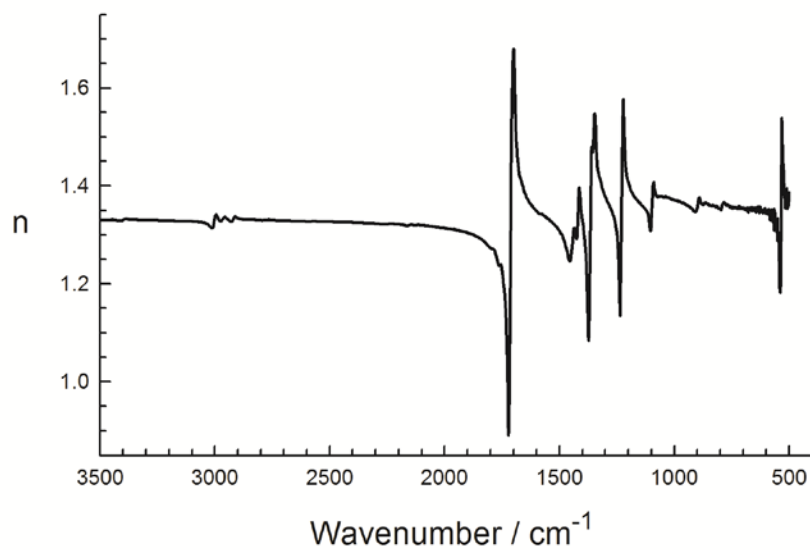


Figure 6. Optical constants for amorphous acetone at 10 K. See <https://science.gsfc.nasa.gov/691/cosmicice/constants.html> for n and k values.

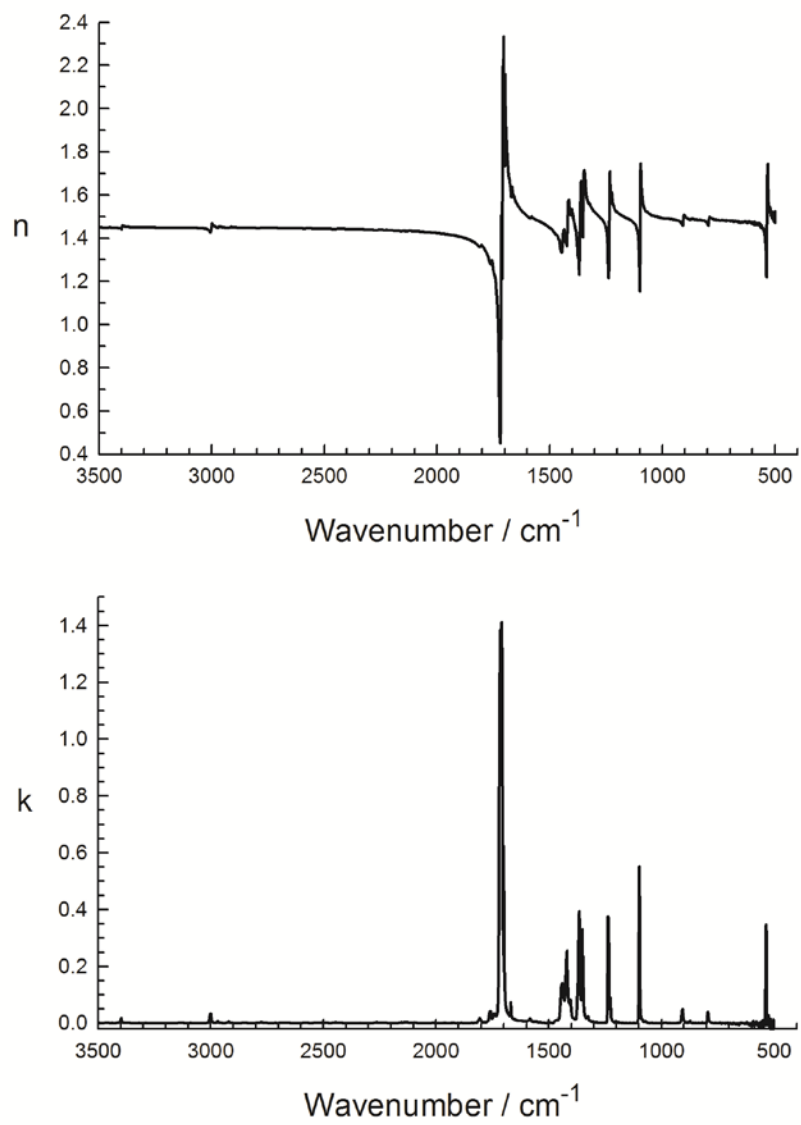


Figure 7. Optical constants for crystalline acetone at 125 K. See <https://science.gsfc.nasa.gov/691/cosmicice/constants.html> for n and k values.

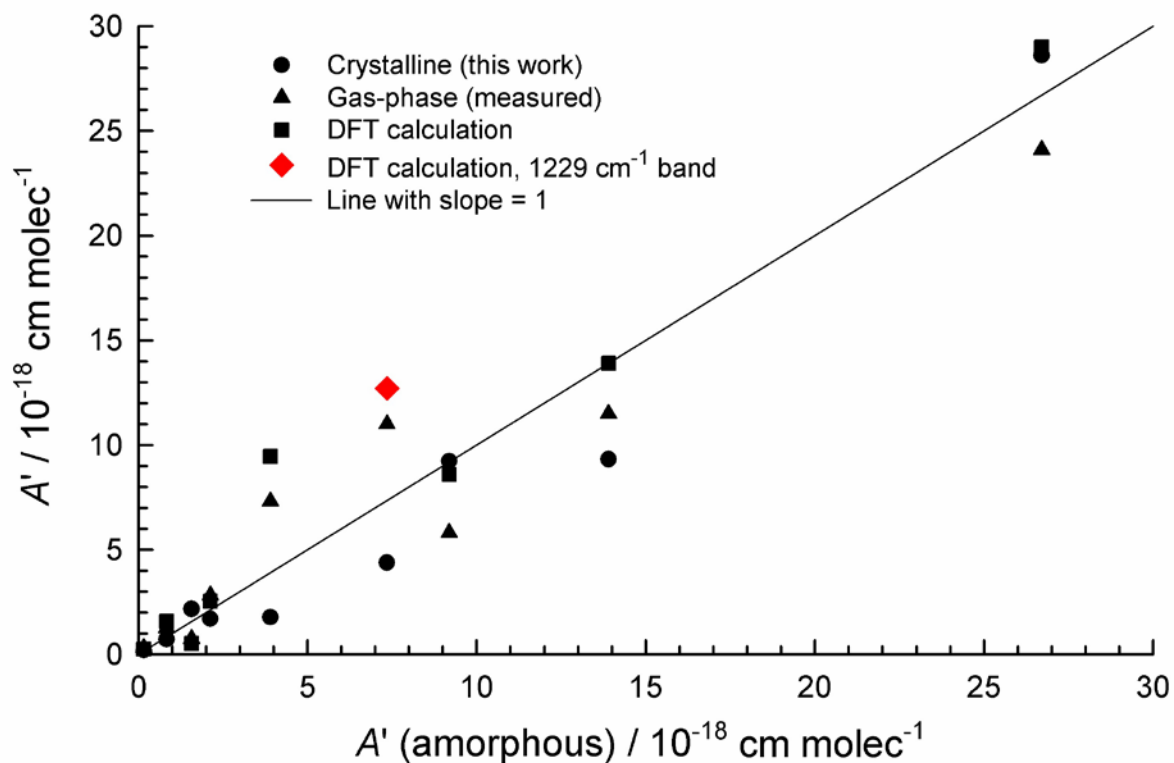


Figure 8. Comparisons of band strengths measured for crystalline acetone (\bullet), measured for gas-phase acetone (\blacktriangle), and calculated for gas-phase acetone (\blacksquare) with those measured for amorphous acetone. The line drawn has a slope of 1. The red diamond (\blacklozenge) is for the DFT value used in reference 4.